Synthesis and evaluation of (-)- and (+)-[(11)C]galanthamine as PET tracers for cerebral acetylcholinesterase imaging.

AUTHOR(S):

Kimura, Hiroyuki; Kawai, Tomoki; Hamashima, Yoshio; Kawashima, Hidekazu; Miura, Kenji; Nakaya, Yuta; Hirasawa, Makoto; ... Ono, Masahiro; Node, Manabu; Saji, Hideo

CITATION:

Kimura, Hiroyuki ...[et al]. Synthesis and evaluation of (-)- and (+)-[(11)C]galanthamine as PET tracers for cerebral acetylcholinesterase imaging.. Bioorganic & medicinal chemistry 2014, 22(1): 285-291

ISSUE DATE:

2014-01-01

URL:

http://hdl.handle.net/2433/180294

Synthesis and Evaluation of (−)- and (+)-[^{11}C]Galanthamine as PET Tracers for Cerebral Acetylcholinesterase Imaging

Hiroyuki Kimura[a,*], Tomoki Kawai[a], Yoshio Hamashima[b], Hidekazu Kawashima[c], Kenji Miura[d], Yuta Nakaya[a], Makoto Hirasawa[a], Kenji Arimitsu[a], Tetsuya Kajimoto[b], Yoshiro Ohmomo[e], Masahiro Ono[a], Manabu Node[b] and Hideo Saji[a,*]

[a]*Department of Patho-Functional Bioanalysis, Graduate School of Pharmaceutical Sciences, Kyoto University, 46-29 Yoshida Shimoadachi-cho, Sakyo-ku, Kyoto 606-8501, Japan*

[b]*Department of Pharmaceutical Manufacturing Chemistry, Kyoto Pharmaceutical University, 1 Shichono-cho, Yamashina-ku, Kyoto 607-8414, Japan*

[c]*Department of Nuclear Medicine and Diagnostic Imaging, Graduate School of Medicine, Kyoto University, 54 Shogoin Kawahara-cho, Sakyo-ku, Kyoto 606-8507, Japan*

[d]*SHI Accelerator Service Ltd., 1-17-6 Osaki, Shinagawa-ku Tokyo 141-0032, Japan*

[e]*Osaka University of Pharmaceutical Sciences, 4-1-20 Nasahara, Takatsuki, Osaka 569-1094,*

Japan

*To whom correspondence should be addressed: Phone: +81-75-753-4566

Fax: +81-75-753-4568

E-mail: hsaji@pharm.kyoto-u.ac.jp

hkimura@pharm.kyoto-u.ac.jp

Abstract

Improved radiopharmaceuticals for imaging cerebral acetylcholinesterase (AChE) are needed for the diagnosis of Alzheimer's disease (AD). Thus, ^{11}C-labeled (−)-galanthamine and its enantiomers were synthesized as novel agents for imaging the localization and activity of AChE by positron emission tomography (PET). C-11 was incorporated into (−)- and (+)-[^{11}C]galanthamine by *N*-methylation of norgalanthamines with [^{11}C]methyl triflate. Simple accumulation of ^{11}C in the brain was measured in an *in vivo* biodistribution study using mice, whilst donepezil was used as a blocking agent in analogous *in vivo* blocking studies. *In vitro* autoradiography of rat brain tissue was performed to investigate the distribution of (−)-[^{11}C]galanthamine, and confirmed the results of PET studies in mice. The radiochemical yields of *N*-methylation of (−)- and (+)-norgalanthamines were 13.7 and 14.4%, respectively. The highest level of accumulation of ^{11}C in the brains of mice was observed at 10 min after administration (2.1% ID/g). Intravenous pretreatment with donepezil resulted in a 30% decrease in accumulation of (−)-[^{11}C]galanthamine in the striatum; however, levels in the

cerebellum were unchanged. In contrast, use of (+)-[^{11}C]galanthamine led to accumulation of radioactivity in the striatum equal to that in the cerebellum, and these levels were unaffected by pretreatment with donepezil. In *in vitro* autoradiography of regional radioactive signals of brain sections showed that pretreatment with either (−)-galanthamine or donepezil blocked the binding of (−)-[^{11}C]galanthamine to the striatum, while sagittal PET imaging revealed accumulation of (−)-[^{11}C]galanthamine in the brain. These results indicate that (−)-[^{11}C]galanthamine showed specific binding to AChE, whereas (+)-[^{11}C]-galanthamine accumulated in brain tissue by non-specific binding. Thus, optically pure (−)-[^{11}C]galanthamine could be a useful PET tracer for imaging cerebral AChE.

Keywords: Acetylcholinesterase inhibitor, Galanthamine, Positron emission tomography tracers, C-11

Graphical abstract

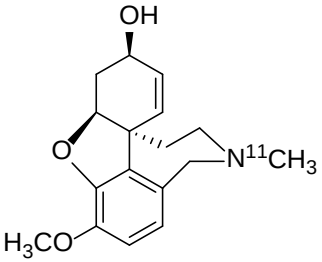

(−)-[^{11}C]galanthamine

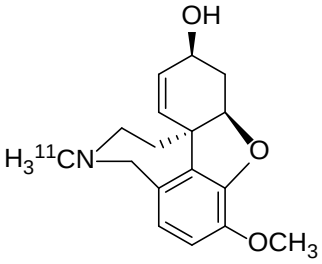

(+)-[^{11}C]galanthamine

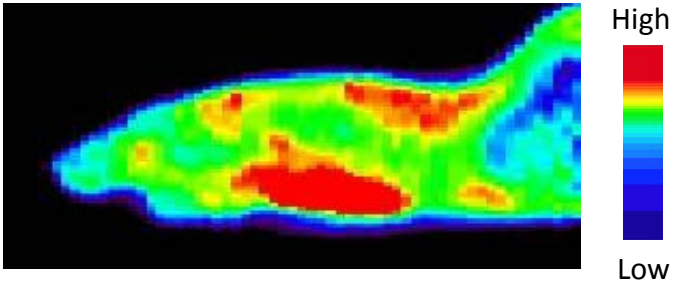

Sagittal PET image of (−)-[^{11}C]galanthamine in the ddY mouse.

1. Introduction

The function of the brain cholinergic system, where acetylcholine (ACh), acetylcholinesterase (AChE) and choline acetyltransferase (ChAT) act to control the potential of nerve cells, is crucial to memory, learning, and recognition. Decreases in the activities of AChE and ChAT have been observed in the brains of patients suffering from Alzheimer's disease (AD), while increased activity of AChE in some regions, for example the hippocampus and striatum, has been correlated with cognitive decline in AD patients.[1] Thus, some AChE inhibitors have been approved for treating mild to moderate AD.

Because noninvasive methods for visualizing AChE levels would be useful for monitoring the treatment and progression of AD, studies have been performed using the substrate-type PET tracer, [^{11}C]MP4A.[2–4] Other derivatives of AChE inhibitors, such as [^{11}C]physostigmine, [^{11}C]methyl-tacrine, and [^{11}C]donepezil, have been developed as radio-tracers specifically binding AChE, and their utility has been evaluated in PET studies.[5–7] Besides donepezil and tacrine, (−)-galanthamine, an alkaloid isolated from

Galanthus woronowii and *Lycoris radiata*, was also developed as a treatment for AD because it showed several biological activities, including allosteric modulation of the nicotinic acetylcholine receptor, and inhibition of AChE.[8] Meanwhile, we have reported a novel synthetic route to (±)-galanthamine and (−)-galanthamine which avoids the use of narwedine (which causes a fatal allergic response in some workers.[9,10]) as an intermediate.

Thus, we examined the potential of (−)- and (+)-[^{11}C]galanthamine (Figure 1) as PET probes in *in vitro* and *in vivo* experiments.

2. Materials and methods

2.1. General

^{1}H and ^{13}C NMR spectra were recorded on a JNM-AL400 spectrometer (JEOL, Tokyo, Japan) with $CDCl_3$ as a solvent and tetramethylsilane (δ 0.00) as an internal standard. Mass spectra (MS) were obtained using a JMS-HX/HX110 A spectrometer (JEOL, Tokyo, Japan). Specific rotations were measured on a p-1020 digital polarimeter (Jasco,

Tokyo, Japan). Silica gel 60N (63–210 μm, Kanto Chemical, Tokyo, Japan) was used for open column chromatography. Silica gel 60 F-254 plates (Merck, Darmstadt, Germany) were used for thin-layer chromatography (TLC). Preparative TLC was performed on silica gel 60 F-254 plates (0.25 mm, Merck) or silica gel 60 F-254 plates (0.5 mm, Merck). All chemicals used were of reagent grade.

2.2. Animal experiments

Experiments were performed on seven-week-old male ddY mice (20–25 g) and nine-week-old male Wistar rats (300 g) in accordance with the institutional guidelines, and the experimental procedures were approved by the Kyoto University Animal Care Committee.

2.3. Synthesis

(±)-Trifluoromethanesulfonyl-*N*-trifluoroacetyl-*N*-nornarwedine (**3**)

Trifluoromethanesulfonic anhydride (1.88 mL, 11.1 mmol) was added to a

solution of (±)-3-hydroxy-*N*-trifluoroacetyl-*N*-nornarwedine (**2**) (665 mg, 1.7 mmol) in pyridine (10 mL) and the reaction mixture was stirred for 75 min at 0°C. Methanol (4 mL) was then added to the mixture, and the organic solvent then removed by evaporation under reduced pressure. The residue was extracted with ethyl acetate, washed with an aqueous solution of sodium bicarbonate (5%), and then brine, dried over magnesium sulfate, and concentrated to dryness *in vacuo*. The residue was purified by silica gel column chromatography (*n*-hexane:acetone = 1:1) to afford compound **3** as colorless crystals (800 mg, 91%). ^{1}H NMR (400 MHz, $CDCl_3$) δ 2.11–2.22 (m, 2H), 2.44 (ddt, *J* = 1.9, 3.5, 14.1 Hz, 1H), 2.79 (dd, *J* = 3.7, 17.8 Hz, 1H), 2.81 (dd, *J* = 3.7, 17.9 Hz, 1H), 3.16 (d, *J* = 17.9 Hz, 1H), 3.17 (d, *J* = 17.9 Hz, 1H), 3.37 (br t, *J* = 13.7 Hz, 0.5H), 3.74 (br t, *J* = 13.7 Hz, 0.5H), 4.00 (s, 1.5H), 4.01 (s, 1.5H), 4.13 (d, *J* = 15.3 Hz, A part of AB type, 0.5H), 4.37 (d, *J* = 16.1 Hz, 0.5H), 4.55 (d, *J* = 16.8 Hz, A' part of A'B' type, 0.5H), 4.77 (d, *J* = 13.7 Hz, 0.5H), 4.83–4.86 (m, 1H), 4.86 (d, *J* = 16.8 Hz, B part of AB type, 1H), 5.24 (d, *J* = 15.4 Hz, B' part of A'B' type, 0.5H), 6.14 (d, *J* = 10.3 Hz, 0.5H), 6.17 (d, *J* = 9.5 Hz, 0.5H), 6.65 (s, 0.5H), 6.79 (d, *J* = 10.6 Hz, 0.5H), 6.80 (d, *J* = 10.6 Hz, 0.5H), 6.82 (s, 0.5H), 6.86 (d, *J* =10.6 Hz, 0.5H), 6.87 (d, *J*

= 10.6 Hz, 0.5H). ^{13}C NMR (100 MHz, $CDCl_3$) δ 34.85, 37.43, 37.48, 46.90, 47.14 (2C), 48.78, 48.83, 51.76, 52.61, 60.99, 61.01, 89.04, 89.16, 115.03, 115.19, 116.09, 117.41 (2C), 117.92, 118.05, 120.61 (2C), 128.04, 128.29, 128.84, 129.03, 131.28, 131.31, 137.71, 137.76, 141.20, 161.27, 141.80, 142.27, 150.65, 150.81, 156.46, 156.66, 156.80, 157.03, 193.44, 193.50. mp 109–111°C. *Anal*. Calcd for $C_{19}H_{15}F_6NO_7S$:C, 44.28; H, 2.93; N, 2.72. Found for $C_{19}H_{15}F_6NO_7S$: C, 44.17; H, 3.02; N, 2.71. HRMS (FAB+) *m/z*: 515.0469 (Calcd for $C_{19}H_{15}F_6NO_7S$:515.0473).

(±)-*N*-Trifluoroacetyl-*N*-nornarwedine (**4**)

Formic acid (99%, 570 μL, 3.52 mmol × 4) was added to a mixture of compound **3** (1.95 g; 3.52 mmol), palladium acetate (18.9 mg, 3.52 mmol × 0.02), 1,1′-bis(diphenylphosphino)ferrocene (dppf) (85 mg, 3.52 mmol × 0.04), and triethylamine (3.3 mL, 3.52 mmol × 6) in DMF (18 mL) at 0°C. The reaction mixture was stirred for 1 h at 60°C and then quenched by pouring into ice-water. The mixture was then filtered and the residue remaining on the filter paper was dissolved in ethyl acetate. The organic layer was washed with brine, dried over magnesium sulfate, and

concentrated to dryness *in vacuo*. The residue was purified by silica gel column chromatography (*n*-hexane:acetone = 1:1) and was further recrystallized from methanol to afford compound **4** as colorless crystals (1.25 g, 97%). ^{1}H NMR (400 MHz, $CDCl_3$) δ 2.09–2.20 (m, 2H), 2.22 (ddt, *J* = 1.8, 3.7, 13.9 Hz, 0.5H), 2.76 (dd, *J* = 3.7, 14.2 Hz, 0.5H), 2.78 (dd, *J* = 3.7, 14.1 Hz, 0.5H), 3.21 (d, *J* = 14.1 Hz, 1H), 3.36 (m, 0.5H), 3.74 (br t, *J* = 13.6 Hz, 0.5H), 3.85 (s, 1.5H), 3.86 (s, 1.5H), 4.15 (d, *J* = 15.1 Hz, 0.5H), 4.36 (br d, *J* = 15.8 Hz, 0.5H), 4.56 (d, *J* = 16.7 Hz, 0.5H), 4.73–4.76 (m, 1H), 4.77 (d, *J* = 16 Hz, 0.5H), 4.91 (br d, *J* = 16.7 Hz, 0.5H), 5.31 (d, *J* = 15.1 Hz, 0.5H), 6.08 (d, *J* = 10.4 Hz, 0.5H), 6.11 (d, *J* = 10.4 Hz, 0.5H), 6.75 (d, *J* = 8.2 Hz, 0.5H), 6.75 (s, 1H), 6.82 (dd, *J* = 2.2, 10.4 Hz, 0.5H), 6.89 (dd, *J* = 2.2, 10.4 Hz, 0.5H), 6.90 (d, *J* = 8.2 Hz, 0.5H). ^{13}C NMR (100 MHz, $CDCl_3$) δ: 35.18, 37.44, 37.50, 38.14, 47.08, 47.26, 47.29, 49.14, 49.19, 52.36, 53.22, 56.40, 56.41, 88.00, 88.12, 112.49, 115.18, 115.31, 118.05, 118.17, 120.91, 121.54, 122.72, 126.46, 126.92, 128.27, 128.45, 129.89, 142.53, 142.53, 142.95, 145.21, 145.26, 147.94, 148.07, 156.34, 156.70, 157.07, 193.99, 194.03. mp 164–165°C. *Anal*. Calcd for $C_{18}H_{16}F_3NO_4$: C, 58.86; H, 4.39; N, 3.81. Found for $C_{18}H_{16}F_3NO_4$: C, 59.13; H, 4.38; N, 3.97. HRMS (FAB+) *m/z*: 367.1035 (Calcd for $C_{18}H_{16}F_3NO_4$: 367.1031).

(±)-Nornarwedine (**5**)

An aqueous solution of sodium hydroxide (2 M, 9 mL) was added to a solution of compound **4** (1.3 g, 3.54 mmol) in methanol (80 mL), and the mixture was stirred for 40 min at room temperature. After the reaction, the organic solvent in the mixture was removed *in vacuo*. The remaining residue was diluted with a saturated aqueous solution of ammonium chloride, and this mixture was extracted with chloroform. The organic layer was concentrated to dryness *in vacuo*, and the residue was purified by silica gel column chromatography (chloroform:methanol = 1:1) to afford compound **5** as colorless crystals (940 mg, 98%). ^{1}H NMR (400 MHz, $CDCl_3$) δ 1.93 (dt, *J* = 3.4, 13.6, 1H), 2.12 (ddd, *J* = 1.8, 3.6, 13.6 Hz, 1H), 2.75 (dd, *J* = 3.7, 17.7 Hz, 1H), 3.16 (ddd, *J* = 0.9, 2.4, 17.7 Hz, 1H), 3.21 (dt, *J* = 1.9, 14.7, 1H), 3.45 (dt, *J* = 3.5, 14.6 Hz, 1H), 3.84 (s, 3H), 4.02 (d, *J* = 15.7 Hz, A part of AB type, 1H), 4.05 (d, *J* = 15.7 Hz, B part of AB type, 1H), 4.73–4.75 (m, 1H), 6.05 (dd, *J* = 0.5, 10.4 Hz, 1H), 6.65 (d, *J* = 8.2 Hz, A part of AB type, 1H), 6.68 (d, *J* = 8.2 Hz, B part of AB type, 1H), 6.94 (dd, *J* = 8.2, 10.4 Hz, 1H). ^{13}C NMR (100 MHz, $CDCl_3$) δ

37.63, 39.93, 47.75, 49.90, 54.38, 56.39, 88.27, 112.04, 121.01, 127.44, 130.98, 133.65, 144.26, 144.94, 147.73, 194.76. Mp.175–176°C. *Anal*. Calcd for $C_{16}H_{17}NO_3$: C, 70.83; H, 6.32; N, 5.16. Found for $C_{16}H_{17}NO_3$: C, 70.56; H, 6.14; N, 5.25. HRMS (FAB+) *m/z*: 272.1283 (Calcd for $C_{16}H_{18}NO_3$: 272.1287).

(±)-Norgalanthamine (**6**)

A solution of lithium tri-*sec*-butylborohydride (L-selectride®) in THF (1M, 12.5 mL) was added to a solution of compound **5** (925 mg, 3.4 mmol) in THF (50 mL) at −78°C, and the resulting mixture was stirred at this temperature for 2 h. Acetone (3 mL) was then added to quench the reaction, and organic solvents in the mixture were then removed *in vacuo*. Methanol (25 mL) was added to the residue to give a precipitate, which was collected by filtration. Recrystallization of this precipitate from methanol gave (±)-norgalanthamine as colorless crystals (780 mg, 84%). ^{1}H NMR (400 MHz, CD_3OD) δ 2.07–2.11 (m, 2H), 2.18 (ddd, *J* = 3.1, 5.3, 15.8 Hz, 1H), 2.51 (d, *J* = 15.8 Hz, 1H), 3.62–3.66 (m, 2H), 3.83 (s, 3H), 4.20 (brt, *J* = 4.8 Hz, 1H), 4.34 (d, *J* = 15.0 Hz, A part of AB type,

1H), 4.54 (d, *J* = 15.0 Hz, B part of AB type, 1H), 4.63 (dt, *J* = 1.3, 3.3 Hz, 1H), 6.02 (ddd, *J* = 1.0, 4.9, 10.3 Hz, 1H), 6.15 (dt, *J* = 1.3, 10.3 Hz, 1H), 6.83 (d, *J* = 8.2 Hz, A part of AB type, 1H), 6.85 (d, *J* = 8.2 Hz, B part of AB type, 1H). ^{13}C NMR (100 MHz, CD_3OD) δ 32.30, 36.77, 47.47, 49.81, 52.58, 57.52, 62.93, 89.43, 114.47, 123.80, 124.41, 127.84, 130.88, 135.06, 147.94, 149.32. mp 235–236°C. *Anal*. Calcd for $C_{16}H_{19}NO_3$: C, 70.31; H, 7.01; N, 5.12; O, 17.56. Found for $C_{16}H_{19}NO_3$: C, 70.25; H, 6.98; N, 5.16; O, 17.43. HRMS (FAB+) *m/z*: 274.1439 (Calcd for $C_{16}H_{19}NO_3$ 274.1443).

(±)-Galanthamine (**1**)

Method A. Sodium cyanoborohydride (20 mg, 0.3 mmol) was added to a solution of (±)-norgalanthamine (27 mg, 0.1 mmol) and 37% formaldehyde (100 µL) in acetic acid (800 µL), and the mixture was stirred for 5 min at room temperature. After this time, the mixture was concentrated to dryness *in vacuo*. The residue was diluted with an aqueous solution of sodium bicarbonate (5%), and this resulting mixture extracted with chloroform. The organic layer was washed with brine, dried over sodium sulfate, and

concentrated to dryness *in vacuo*. The residue was purified by silica gel column chromatography (chloroform:methanol = 5:1) to afford (±)-galanthamine as colorless crystals (25 mg, 92%).

Method B. Methyl triflate (227 μL, 2.0 mmol) was added to a solution of (±)-norgalanthamine (28 mg, 0.1 mmol) and cesium carbonate (665 mg, 2.0 mmol) in DMSO (1.5 mL) in a sealable tube. The tube was sealed, and then stirred for 5 min at 170℃. After this time, the mixture was neutralized with sodium bicarbonate and extracted with chloroform. The organic layer was washed three times with brine, dried over sodium sulfate, and concentrated to dryness *in vacuo*. The residue was purified by silica gel column chromatography (chloroform:methanol = 5:1) to afford (±)-galanthamine as colorless crystals (10 mg, 33%). ^{1}H NMR (400 MHz, $CDCl_3$) δ 1.58 (ddd, *J* = 1.8, 4.0, 13.7 Hz, 1H), 2.01 (ddd, *J* = 1.8, 3.5, 15.7 Hz, 1H), 2.09 (dt, *J* = 3.1, 13.4 Hz, 1H), 2.42 (s, 3H), 2.44 (br s, OH), 2.69 (ddd, *J* = 1.5, 3.3, 15.7 Hz, 1H), 3.05 (br d, *J* = 13.7 Hz, 1H), 3.27 (dt, *J* = 1.7, 13.7 Hz, 1H), 3.69 (dd, *J* = 1.1, 15.2 Hz, A part of AB type, 1H), 3.83 (s, 3H), 4.09 (d, *J* = 15.2 Hz, B part of AB type, 1H), 4.61 (br, 1H), 6.00 (ddd, *J* = 1.2, 4.0, 10.2 Hz,

1H), 6.07 (d, *J* = 1.2, 10.2 Hz, B part of AB type, 1H), 6.62 (d, *J* = 8.2 Hz, A part of AB type, 1H), 6.66 (d, *J* = 8.2 Hz, B part of AB type, 1H). ^{13}C NMR (100 MHz, $CDCl_3$) δ: 30.29, 34.20, 42.52, 48.57, 54.21, 56.24, 61.01, 62.44, 89.09, 111.50, 122.38, 127.94, 127.23, 129.77, 133.43, 144.43, 146.15. mp 122–123°C. *Anal*. Calcd for $C_{17}H_{21}NO_3$: C, 71.06; H, 7.37; N, 4.87. Found for $C_{17}H_{21}NO_3$: C, 70.88; H, 7.23; N, 4.99. HRMS (FAB+) *m/z*: 288.1605 (Calcd for $C_{17}H_{22}NO_3$ 288.1600).

(−)- and (+)-Galanthamine

A solution of (+)- and (−)-norgalanthamine (0.46 mg), cesium carbonate (12.06 mg), and methyl triflate (4 μL) in DMSO (50 μL) was added to a sealable tube, which was then sealed, and the reaction mixture was stirred for 5 min at 170°C. The reaction mixture was analyzed using an HPLC system equipped with a Chiralcel IC column (4.6 × 250 mm, Daicel, Tokyo, Japan), and was separated using a mix of solvents (methyl *t*-butyl ether:ethanol:diethylamine 95:5:0.1) on the same system, at a flow rate of 1.0 mL/min. The retention times of (+)- and (−)-galanthamine, which were detected by UV

absorption at 254 nm, were 12.7 min ($[\alpha]_D^{18}$ = +141.62° (*c* 0.68, ethanol)) and 14.4 min ($[\alpha]_D^{18}$ = −125.99° (*c* 0.66, ethanol)), respectively .

2.4. Optical resolution

The optical resolution of (±)-norgalanthamine was performed on an HPLC system equipped with a Chiralcel IC column (10 × 250 mm, Daicel) with a mobile phase consisting of *n*-hexane, ethanol, and diethylamine (70:30:0.1), which was run at a flow rate of 5.0 mL/min at 30℃. The elution of the two enantiomers was detected by UV absorption at 254 nm, with (+)- and (−)-norgalanthamine obtained as colorless crystals. The retention times of (+)- and (−)-norgalanthamine were 32.5 min ($[\alpha]_D^{24}$ = +71.2^o (*c* 0.29, $CHCl_3$)) and 38.7 min ($[\alpha]_D^{25}$ = −71.0^o (*c* 0.29, $CHCl_3$)), respectively.[11]

2.5. Radiolabeling

^{11}C was prepared by a $^{14}N(p, \alpha)^{11}C$ reaction using a cyclotron system (CYPRIS model 325R, Sumitomo Heavy Industries Ltd., Tokyo, Japan) in Kyoto University

Hospital, and [^{11}C]methyl triflate was synthesized according to the Jewett method.[12] Specifically, $^{11}CO_2$ dissolved in THF was reduced to [^{11}C]methanol with lithium aluminum hydride. [^{11}C]Methanol was reacted with hydrogen iodide to produce [^{11}C]methyl iodide, which was then converted to [^{11}C]methyl triflate by passage through a silver triflate column. [^{11}C]Methyl triflate was reacted with either (−)-norgalanthamine or (+)-norgalanthamine (2 mg/mL, 160 μL) in DMSO, with the mixture being vortexed and heated at 170℃ for 5 min. The reaction mixture was purified using an HPLC system equipped with a Cosmosil 5C_{18}-MS-II column（10 × 250 mm, Nacalai, Kyoto, Japan) using a mobile phase consisting of water, acetonitrile, and diisopropylamine (77:23:0.2) at a flow rate of 4 mL/min. The desired product was detected by UV absorption at 254 nm. The retention time of (−)- and (+)-[^{11}C]galanthamine was 13.9 min, while that of (−)- and (+)-norgalanthamine was 7.5 min. The radiochemical purity of the labeled compounds was determined by analytical HPLC using the conditions described above.

2.6. Measurement of AChE Activity

The inhibitory activities of (−)- and (+)-galanthamine against AChE were measured using a modified version of the colorimetric method of Ellman.[13] Thus, 2 µL of a 10-mM solution of inhibitor in 0.1 M phosphate buffer (pH 8) was mixed with 190 µL of AChE solution (extracted from the brain tissue of a 9-week-old rat) in each well of a 96-well titer plate. After the incubation of the titer plate for 30 min at 37℃, 600 µL of 10-mM 5,5'-dithiobis-(2-nitrobenzoic acid) (DTNB), 100 µL of 150-mM acetylthiocholine iodide and 100 µL of buffer were successively added. Changes in UV absorbance of the reaction mixture were then measured at 2 min intervals in a 96-well plate reader at 415 nm, three times, consecutively. Percentage inhibition was calculated by comparison with that for the control (phosphate buffer).

$$\text{Inhibition (\%)} = (1 - A_{\text{inhibitor}}/A_{\text{control}}) \times 100$$

(−)-Galanthamine hydrobromide from *Lycoris* sp. (Sigma) served as a positive indicator for measuring the inhibition of the synthesized (−)- and (+)-galanthamines.

2.7. Biodistribution studies

Either (−)-[^{11}C]galanthamine or (+)-[^{11}C]galanthamine (3.7 MBq each) was administered to seven-week-old male ddY mice. Five animals were then sacrificed by exsanguination at time-points of 2, 5, 15, 30, and 60 min post-administration. The excised blood and brain (or brain tissues, *i.e.*, striatum and cerebellum) were weighed, and the radioactivities of the organs were measured using an auto-well gamma counter (Cobra Auto-Gamma Counter 5003, Packard, Meriden, CT, USA). Radioactivity levels of the organs are expressed as the percentage of injected dose per gram of tissue (% ID/g).

As in *in vivo* blocking studies, mice were pre-treated with donepezil (1.2, 2.3, and 4.6 mg/kg) via tail-vein injection 30 min before administration of (−)- or (+)-[^{11}C]galanthamine. Ten minutes after administration of radioactive [^{11}C]galanthamine, the accumulation of radioactivity to the brain tissue was measured.

2.8. In vitro autoradiographic experiments

In vitro autoradiography was performed on 20-µm coronal brain sections from male Wistar rats. The sections were thaw-mounted onto precleaned silane-coated slides, and incubated with (−)-[^{11}C]galanthamine (2.2 MBq/200 µL) in a binding buffer for 30 min at 4°C. After washing with ice-cold binding buffer and ice-cold water, the slides were placed on Fuji imaging plates (BAS-SR, Fujifilm Photo Film, Tokyo, Japan) for 6 h, together with calibrated ^{11}C-labeled external standards.

As in *in vitro* blocking experiments, brain tissues were incubated with (−)-[^{11}C]galanthamine in the presence of 10 mM (−)-galanthamine or 20 µM donepezil. The images were analyzed using a bio-imaging analyzer (BAS5000, Fujifilm Photo Film, Tokyo, Japan) and Image Gauge software (Fujifilm Photo Film).

2.9. PET studies

PET studies were performed using a GE Healthcare eXplore VISTA PET camera (GE Healthcare, Little Chalfont, UK). A seven-week-old male ddY mouse (20–25 g) was anesthetized (1.5% isoflurane) and (−)-[^{11}C]galanthamine (74 MBq, in

0.2 mL isotonic saline) was injected via the tail vein. Emission data from the animal were then collected for 10–30 min. The images were reconstructed using a 2-D ordered-set expectation-maximization algorithm.

2.10. Statistical analysis

Data are expressed as means ± SD. The statistical significance of differences was evaluated using the Tukey–Kramer test. A value of $p < 0.05$ was considered significant.

3. Results

3.1. Synthesis of galanthamine

The synthetic routes to (±)-galanthamine (**1**) and (±)-norgalanthamine (**6**) are shown in Scheme 1. (±)-3-Hydroxy-*N*-trifluoroacetyl-*N*-nornarwedine (**2**)[9,10] was converted to triflate **3** by a conventional method, and subsequent reduction of **3** with formic acid in the presence of palladium acetate and dppf gave narwedine derivative **4**.

The trifluoroacetamide group of **4** was cleaved by hydrolysis with methanolic sodium hydroxide to afford the amine **5**. Subsequent diastereoselective reduction of **5** with L-selectride® gave (±)-norgalanthamine (**6**) in good yield (84%). An alternative *N*-methylation of **5** was attempted using methyl iodide or methyl triflate as the methylating agent. However, the former conditions gave no product, while the latter conditions provided only a low yield of (±)-galanthamine (33%). The overall yield of (±)-galanthamine from **2** was 25%.

(±)-Norgalanthamine (**6**) could be separated into optically pure (+)- and (−)-**6** using an HPLC system equipped with a chiral column.

3.2. Radiolabeling of (−)- and (+)-[^{11}C]galanthamine

Both (−)- and (+)-[^{11}C]galanthamine were synthesized according to the route shown in Scheme 2. The radiochemical yields of (−)- and (+)-[^{11}C]galanthamine from (−)- and (+)-**6** were 13.7 and 14.4%, respectively, and their radiochemical purities were >99%. No significant difference in [^{11}C]-labeling efficiency of the enantiomers was

observed (Scheme 2).

3.3. Measurement of AChE Activity

The AChE-inhibitory activities of (–)- and (+)-galanthamine are shown in Table 1. Percentage inhibition was measured by the Ellman method. Naturally occurring and synthesized (–)-galanthamine showed similar potent inhibition of AChE (95 ± 1.0% and 94 ± 2.7%, respectively), while (+)-galanthamine exhibited only weak inhibition (10 ± 4.4%).

3.4. Biodistribution studies

The distributions of (−)- and (+)-[^{11}C]galanthamine are summarized in Figure 2. Both (−)- and (+)-[^{11}C]galanthamine rapidly penetrated the brain. The highest levels of radioactive galanthamine in the brain were observed at 10 min post-injection (2.1% ID/g for both compounds), at which point the brain:blood ratios of the compound were ~1.5:1.0.

The regional distribution of radioactivity in the mouse brain is shown in Figure 3. Accumulation of (−)-[^{11}C]galanthamine was greater in the striatum (2.1% ID/g, AChE-rich region) than in the cerebellum (1.7% ID/g, an AChE-poor region). In contrast, there was no difference in accumulation of (+)-[^{11}C]galanthamine in these region (i.e., 1.5% ID/g for the striatum; 1.5% ID/g for the cerebellum).

Pretreatment with donepezil had no effect on striatal accumulation of (+)-[^{11}C]galanthamine, but did lead to a significant decrease in accumulation of (−)-[^{11}C]galanthamine (i.e. dose-dependently, to the basal level (1.3% ID/g, 4.6 mg/kg)).

3.5. In vitro autoradiographic experiments

In vitro autoradiographic analyses were performed (Figure 4) to investigate the regional distribution of (−)-[^{11}C]galanthamine in the brain in more detail. The radioactivity level was the highest in the striatum (Fig. 4b), consistent with the distribution of AChE observed in immunostaining (Fig. 4a). Furthermore, the effects of

(−)-galanthamine (10 mM) (Fig. 4c) and donepezil (20 μM) (Fig. 4d) on the striatal uptake of (−)-[^{11}C]galanthamine were studied. Striatal accumulation of (−)-[^{11}C]galanthamine significantly decreased in the presence of galanthamine or donepezil (Fig. 4e).

3.6. PET studies

Sagittal PET imaging of mouse brain revealed the localization of (−)-[^{11}C]galanthamine in the striatum (Fig. 5), which coincided with the localization of AChE in the brain as determined by immunostaining and *in vitro* autoradiography.

4. Discussion

Because the half-life time of ^{11}C is very short (~20 min), the ^{11}C-containing moiety should be incorporated in the final step of preparation of the target compound. Accordingly, we developed a synthetic pathway using a facile *N*-methylation of norgalanthamine with [^{11}C]methyl triflate. The required (±)-norgalanthamine precursor

was synthesized efficiently in good overall yield (Scheme 1), and it was important to conduct the *N*-Methylation of (±)-norgalanthamine to (±)-galanthamine within a short time-period. An alternative route to **6** via reductive methylation of **5** was not explored, due to the difficulty in preparing and handling the required [^{11}C]formaldehyde.

The synthesized (−)-norgalanthamine [(−)-**6**] was identified by comparing its spectroscopic and specific rotation data with analogous data of an authentic sample of (−)-**6**[14] obtained by chiral HPLC resolution of (±)-norgalanthamine. Chiral HPLC also showed that methylation of (−)-**6** produced only (−)-galanthamine, meaning that (−)- and (+)-[^{11}C]galanthamine were obtained from their respective precursors with radiochemical yields of 13.7 and 14.4%, respectively, and radiochemical purities >99%.

In vitro experiments indicated that (−)-galanthamine had inhibitory activity against AChE comparable with the activity of commercially available (−)-galanthamine hydrobromide, while (+)-galanthamine was only weakly active.

In the study of the biodistribution of (−)- and (+)-[^{11}C]galanthamine in normal mice, the total uptake amount of each isomer in brain was almost the same, which

meant that the chirality of galanthamine had no effect on its ability to penetrate the blood–brain barrier.

In regional distribution studies in normal mouse brains, accumulation of (−)-[^{11}C]galanthamine was greater in the striatum than in the cerebellum. It is considered that these differences reflect the distribution of AChE in brain tissue.[7,15] Meanwhile, the difference in the accumulation of (+)-[^{11}C]galanthamine in these regions was not significant. Accumulation of (−)-[^{11}C]galanthamine significantly decreased after *in vivo* donepezil pretreatment; however, accumulation of (+)-[^{11}C]galanthamine was unaffected. Incomplete blockade of striatal (−)-[^{11}C]galanthamine accumulation by pre-injection of a fatal dose of donepezil (4.6 mg/kg) may represent nonspecific binding to brain tissues.

The slightly higher lipophilicity of (−)- and (+)-[^{11}C]galanthamine (log P = 1.41, as calculated with ChemBioDraw Ultra 12.0) may explain the significant nonspecific accumulation of these compounds in the cerebellum, despite the low levels of AChE in this area of the brain.

In addition, it is reported that (−)-galanthamine not only inhibits AChE, but also binds to α7 or α4β2 nicotinic acetylcholine receptors (AChRs), and allosterically stimulates the pharmacological action of acetylcholine.[16,17] Because donepezil possesses affinity for muscarinic M1 AChRs,[18] but not for nicotinic AChRs, striatal radioactivity after the donepezil-blockade can include the binding of (−)-[^{11}C]galanthamine to nicotinic AChRs.

Autoradiographic analyses demonstrated that (−)-[^{11}C]galanthamine, as detected by immunostaining, accumulated within AChE-abundant regions of the brain, and its accumulation was significantly decreased by pre-treatment of animals with donepezil. These results indicate that (−)-[^{11}C]galanthamine bound to AChE. The fact that both (−)-galanthamine and donepezil did not completely block the accumulation of (−)-[^{11}C]galanthamine in the striatum can be explained by the lipophilicity of the latter, as discussed above.

PET imaging of mice injected with [^{11}C]galanthamine showed greater localization of radioactivity in the striatum than in the cerebellum. This is considered to

support the data of the *in vivo* biodistribution study and the *in vitro* autoradiographic experiment. The results indicate that (−)-[^{11}C]galanthamine satisfies the basic requirements for a radiotracer, and that it could be a potential PET tracer for AChE expression.

Our PET analyses did not include blocking studies using donepezil or other ligands targeting the brain cholinergic system; however, (−)-galanthamine is a therapeutic drug in clinical use for AD patients and the pharmacologic binding site is well defined. The targets of (−)-galanthamine are: 1) AChE and 2) nicotinic AChR (as an allosteric potentiating ligand). From this point of view, experiments to demonstrate how AChE concentration actually contributes to brain PET images should be studied using AD model animals. Further comparison with other binding-type AChE PET tracers, such as [^{11}C]donepezil,[7] may also provide new insights into AD pathology. Relative potency of AChE inhibition (Ki) for donepezil was 3- to 15-fold higher than that for galantamine,[19] suggesting that (−)-[^{11}C]galanthamine itself has lower affinity for AChE compared with [^{11}C]donepezil. The low affinity is unfavorable for AChE

imaging by (−)-[^{11}C]galanthamine; however, different images derived from the different binding properties of those two tracers, i.e., [^{11}C]donepezil and (−)-[^{11}C]galanthamine, could shed new light on the pathogenesis and progression of AD.

5. Conclusion

We have devised a simple synthetic method for generating (−)- and (+)-[^{11}C]galanthamine, and evaluated their potential as PET tracers for imaging the level and activity of AChE in murine brain tissue. The results indicate that (−)-[^{11}C]galanthamine shows radioactive signals which include specific binding to AChE, whereas (+)-[^{11}C]galanthamine only shows radioactive signals representative of non-specific binding. This means that signals derived solely from (−)-[^{11}C]galanthamine can be used to indicate the amount of AChE.

(−)-[^{11}C]Galanthamine thus satisfies the basic requirements for a potential PET tracer for imaging the amount and activity of AChE. The characteristics of (+)-[^{11}C]galanthamine may also provide useful information for the development of

practical radiopharmaceuticals as PET tracers for cerebral AChE imaging.

Acknowledgments

This work was supported in part by a Grant-in-Aid for General Scientific Research from the Japan Society for the Promotion of Science. No other potential conflict of interest relevant to this article was reported.

References

1. Perry, E. K.; Tomlinson, B. E.; Blessed, G.; Bergmann, K.; Gibson, P. H.; Perry, R. H. *Br. Med. J.* **1978**, *2*, 1457.

2. Bormans, G.; Sherman, P.; Snyder, E.; Kilbourn, M. R. *Nucl. Med. Biol.* **1996**, *23*, 513.

3. Irie, T.; Fukushi, K.; Namba, H.; Iyo, M.; Tamagami, H.; Nagatsuka, S.; Ikota, N. *J. Nucl. Med.* **1996**, *37*, 649.

4. Marcone, A.; Garibotto, V.; Moresco, R. M.; Florea, I.; Panzacchi, A.; Carpinelli, A.; Virta, J. R.; Tettamanti, M.; Borroni, B.; Padovani, A.; Bertoldo, A.; Herholz, K.; Rinne, J. O.; Cappa, S. F.; Perani, D. *J. Alzheimers Dis.* **2012**, *31*, 387.

5. Tavitian, B.; Pappata, S.; Planas, A. M.; Jobert, A.; Bonnot-Lours, S.; Crouzel, C.; Di Giamberardino, L. *Neuroreport* **1993**, *4*, 535.

6. Bonnotlours, S.; Crouzel, C.; Prenant, C.; Hinnen, F. *J. Label. Compd. Radiopharm.* **1993**, *33*, 277.

7. Funaki, Y.; Kato, M.; Iwata, R,; Sakurai, E.; Sakurai, E.; Tashiro, M.; Ido, T.; Yanai,

K. *J. Pharmacol. Sci.* **2003**, *91*, 105.

8. Bores, G. M.; Huger, F. P.; Petko, W.; Mutlib, A. E.; Camacho, F.; Rush, D. K.; Selk, D. E.; Wolf, V.; Kosley, Jr., R. W.; Davis, L.; Vargas, H. M. *J. Pharmacol. Exp. Ther.* **1996**, *277*, 728.

9. Node, M.; Kodama, S.; Hamashima, Y.; Baba, T.; Hamamichi, N.; Nishide, K. *Angew. Chem. Int. Ed.* **2001**, *40*, 3060.

10. Node, M.; Kodama, S.; Hamashima, Y.; Katoh, T.; Nishide, K.; Kajimoto, T. *Chem. Pharm. Bull.* **2006**, *54*, 1662.

11. Forgo, P.; Hohmann, J. *J. Nat. Prod.* **2005**, *68*, 1588.

12. Jewett, D. M. *Appl. Radiat. Isot.* **1992**, *43*, 1383.

13. Ellman, G. L.; Courtney, D.; Andies, V.; Featherstone, R. M. *Biochem. Pharmacol.* **1961**, *7*, 88.

14. See also: US patent US20060069251A1 and CAS Number 41303-74-6.bd

15. Tavitian, B.; Pappata, S.; Bonnot-Lours, S.; Prenant, C.; Jobert, A.; Crouzel, C.; Di Giamberardino, L. *Eur. J. Pharmacol.* **1993**, *236*, 229.

16. Samochocki, M.; Höffle, A.; Fehrenbacher, A.; Jostock, R.; Ludwig, J.; Christner, D.; Radina, M.; Zerlin, M.; Ullmer, C.; Pereira, E. F. R.; Lubbert, H.; Albuquerque, E. X.; Maelicke, A. *J. Pharmacol. Exp. Ther.* **2003**, *305*, 1024.

17. Lanctôt, K. L.; Rajaram, R. D.; Herrmann, N. *Ther. Adv. Neurol. Disord.* **2009**, *2*, 163.

18. Snape, M. F.; Misra, A.; Murray, T. K.; De Souza, R. J.; Williams, J. L.; Cross, A. J.; Green, A. R. *Neuropharmacology* **1999**, *38*, 181.

19. Geerts, H.; Guillaumat, P-O.; Grantham, C.; Bode, W.; Anciaux, K.; Sachak, S. *Brain Res.* **2005**, *1033*, 186.

Figure 1.

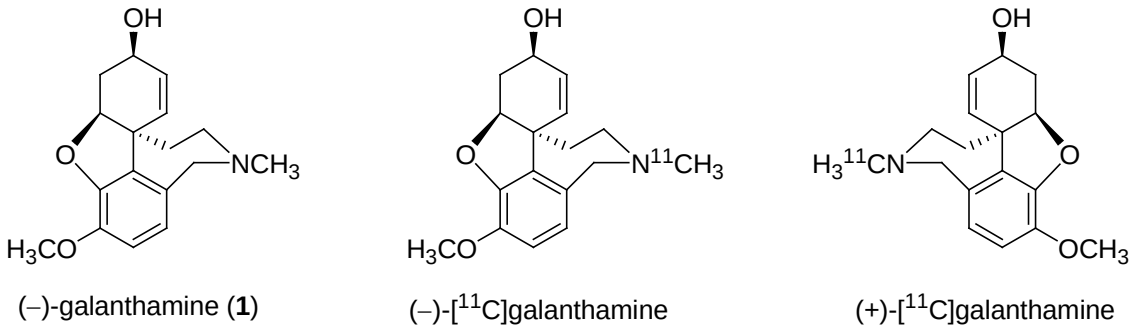

Fig. 1. Chemical structures of (−)-galanthamine, (−)- and (+)-[^{11}C]galanthamine.

Figure 2.

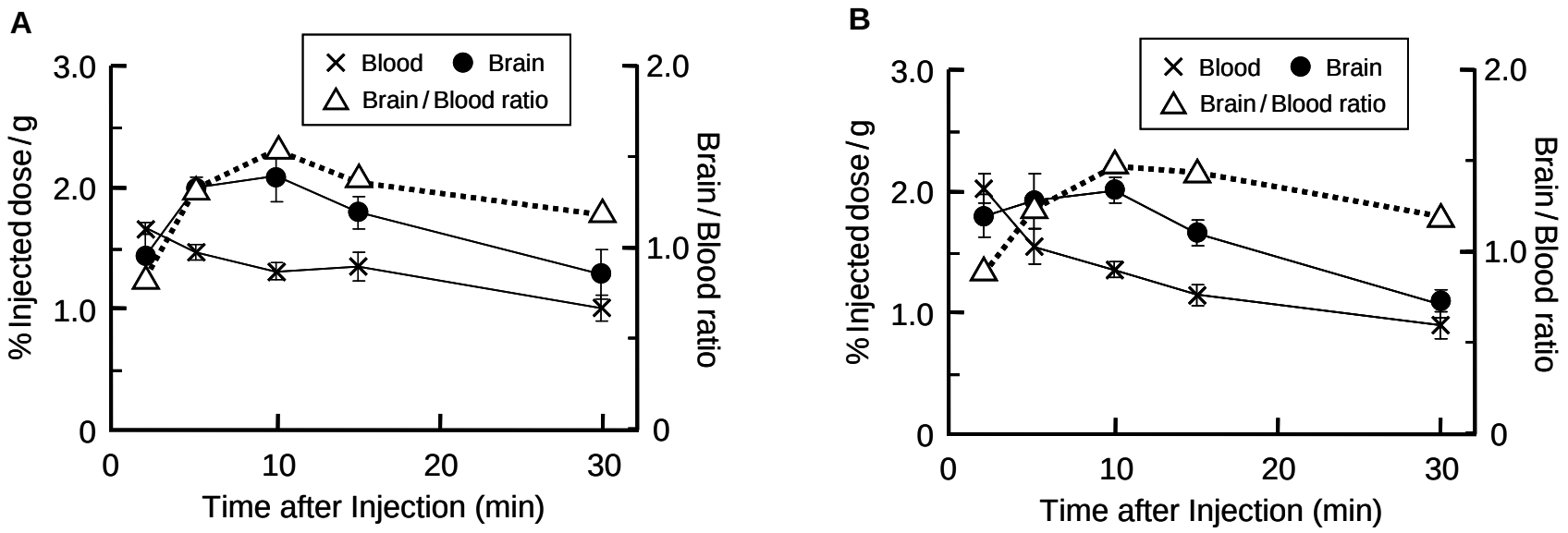

Fig. 2. Brain and blood levels of (−)-[^{11}C]galanthamine (**A**) and (+)-[^{11}C]galanthamine (**B**) in ddY mice. Values representing % injected dose/gram tissue are means ± s.d. (n = 5). The brain/blood ratios are also shown (broken line).

Figure 3.

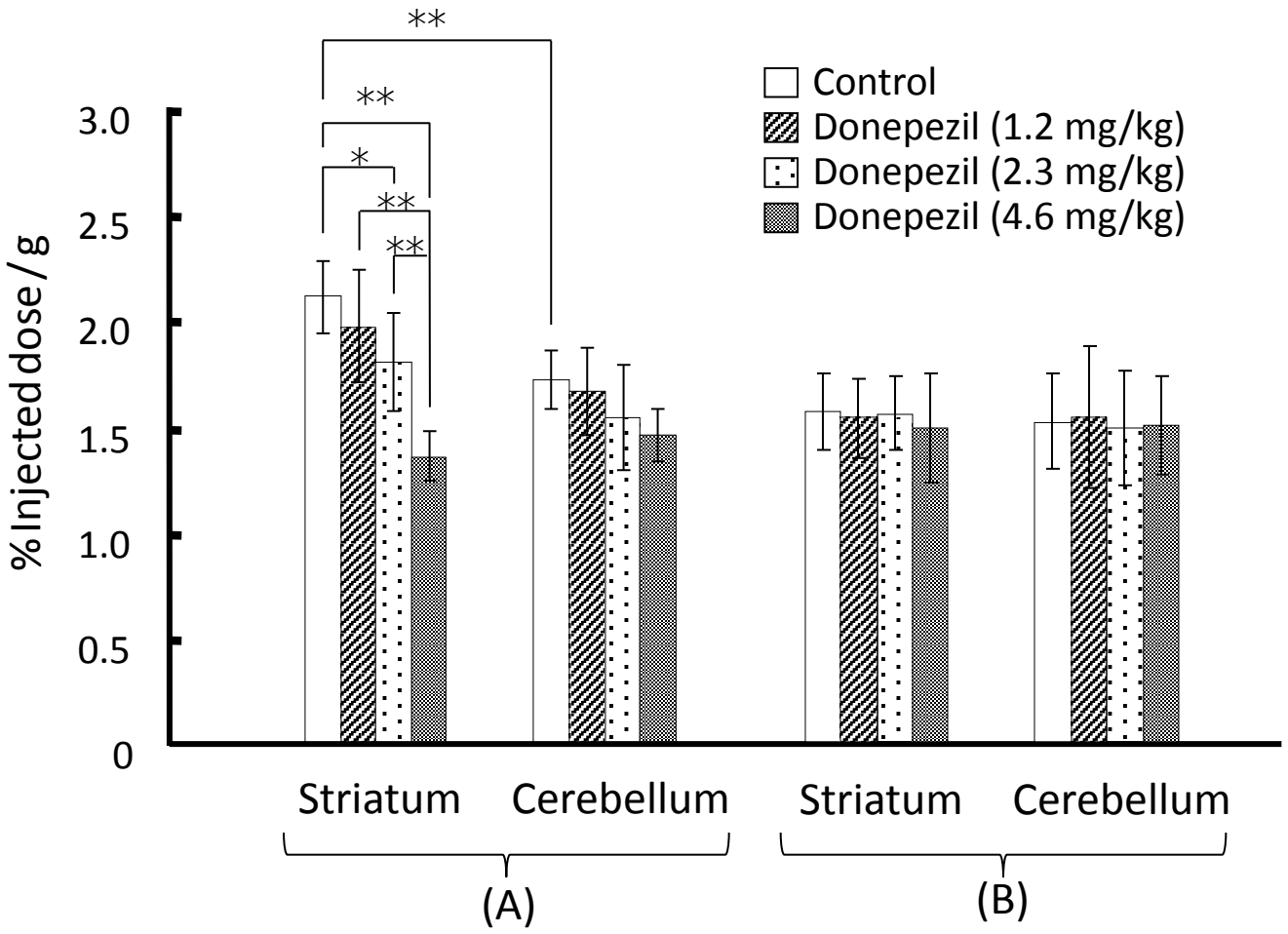

Fig. 3. Effect of different dosages of donepezil on the uptake of (−)-[^{11}C]galanthamine (A) and (+)-[^{11}C]galanthamine (B) in two brain regions of mice. Both (−)- and (+)-[^{11}C]galanthamine were administered intravenously (i.v.), 30 min after i.v. donepezil treatment [where * $p < 0.05$; ** $p < 0.01$ (vs. control)].

Figure 4.

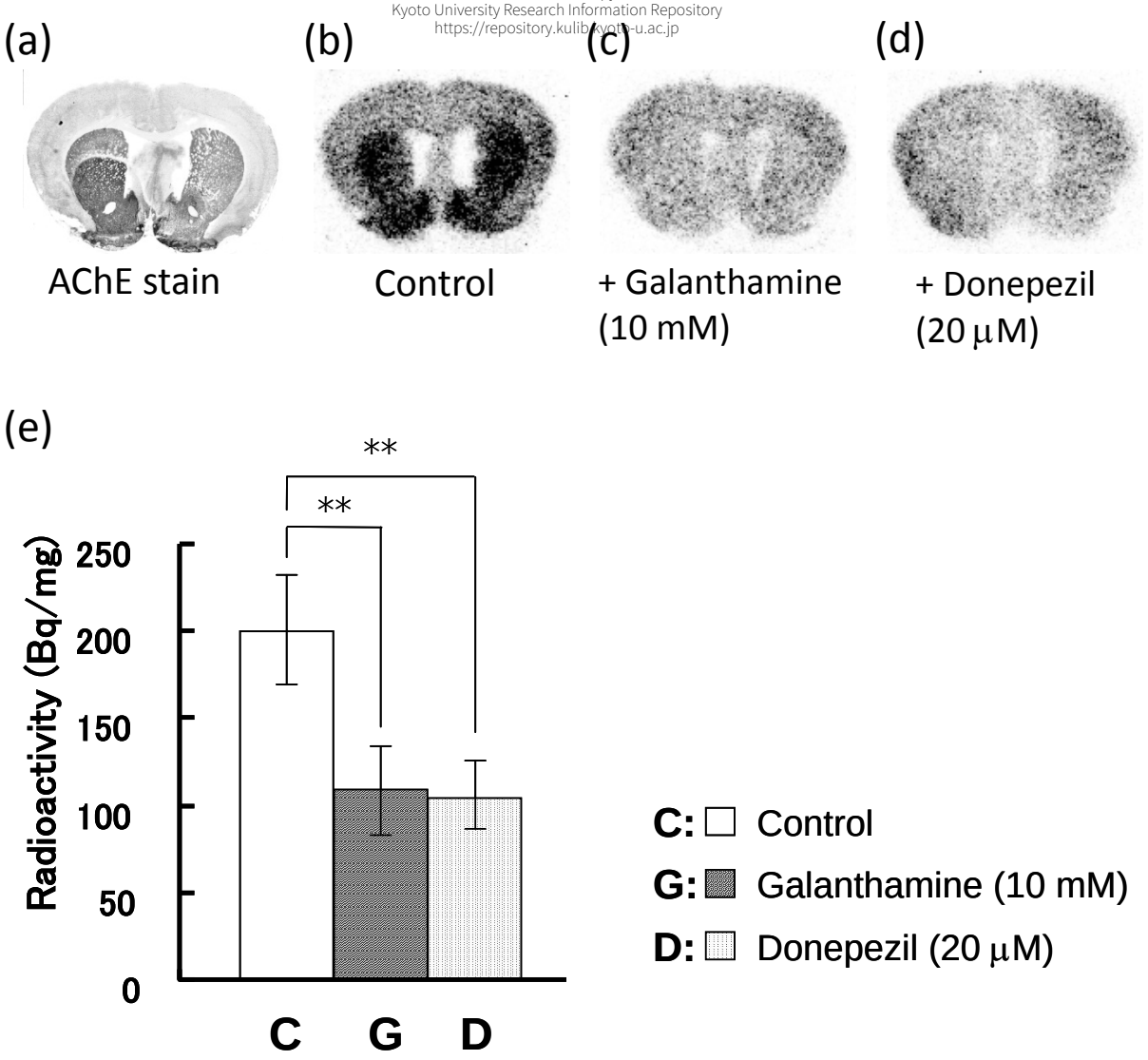

Fig. 4. Accumulation of (−)-[^{11}C]galanthamine in rat brain sections as determined by *in vitro* autoradiography, with: AChE staining of a rat coronal brain section (a); representative *in vitro* autoradiograms of rat coronal brain sections at 30 min after incubation of (−)-[^{11}C]galanthamine (b), with galanthamine (10 mM) (c), or donepezil (20 μM) (d); illustration of the significant decrease in accumulation of (−)-[^{11}C]galanthamine in the presence of galanthamine or donepezil (e) (where ** $p < 0.01$ vs. control).

Figure 5.

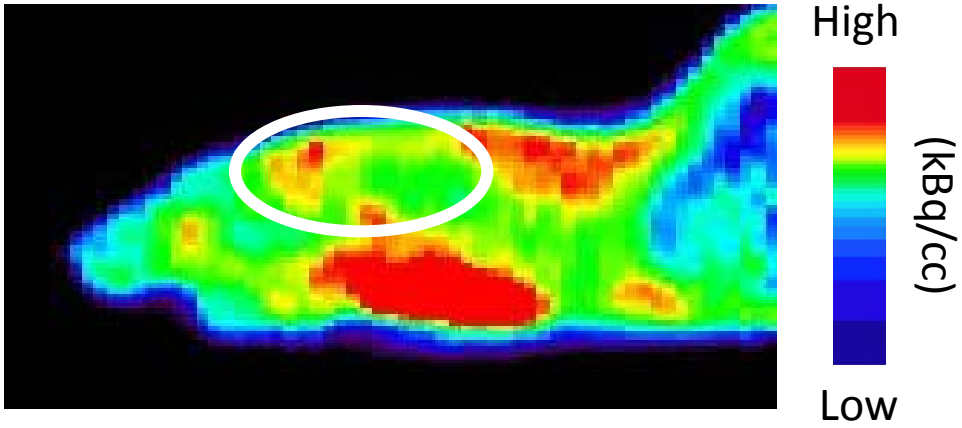

Fig. 5. Sagittal PET image of (−)-[^{11}C]galanthamine in the ddY mouse. The region surrounded by the ellipse indicates the location of the brain.

Scheme 1.

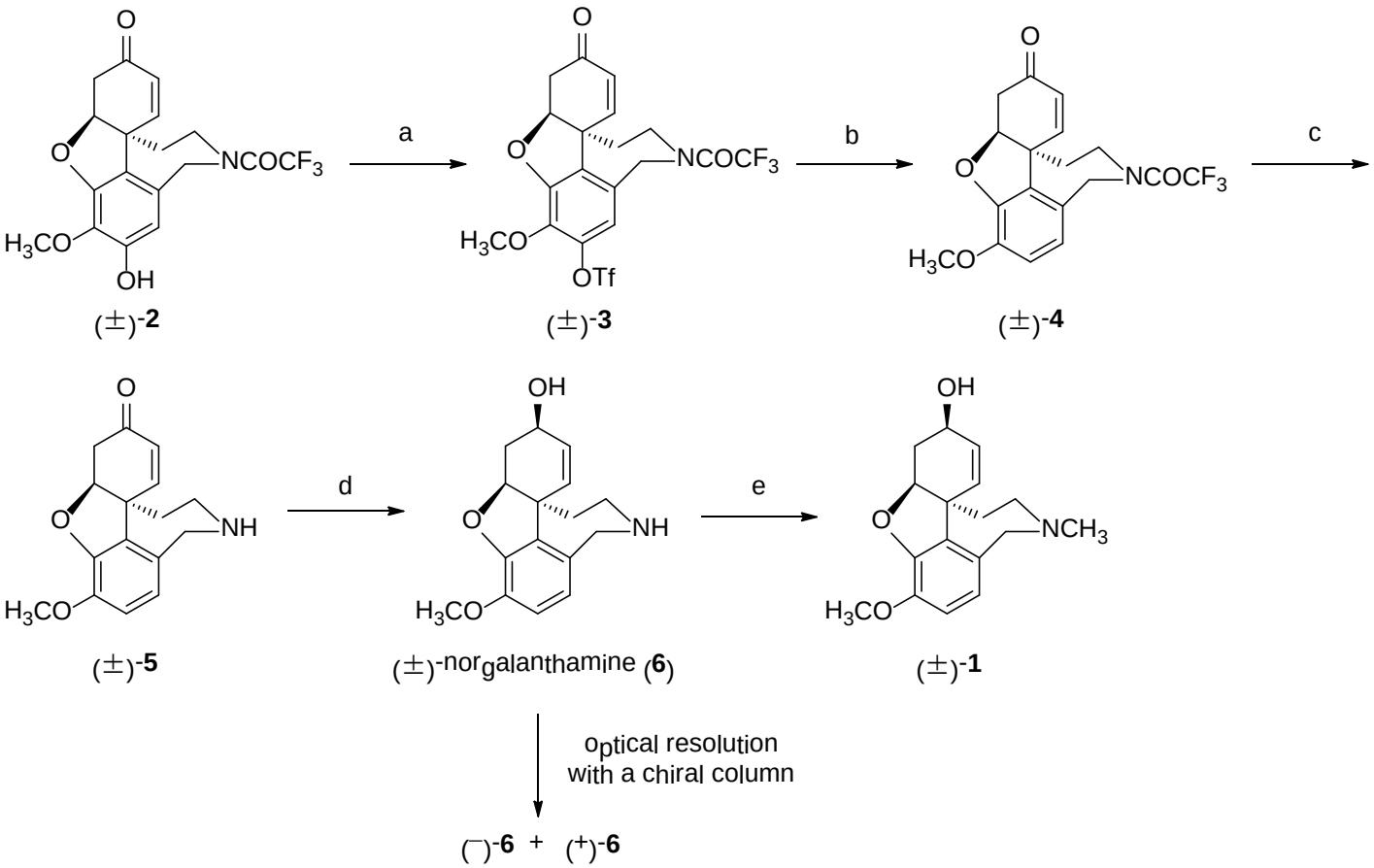

a: Tf_2O, pyridine, 0 °C, 91%, b: $Pd(OAc)_2$, dppf, Et_3N, HCO_2H, DMF, 60 °C, 97%, c: NaOH, MeOH, rt, 98%, d: L-Selectride, THF, −78 °C to rt, 84%, e: (method A) HCHO, $NaBH_3CN$, CH_3CO_2H, rt, 5 min, 92%, (method B) CH_3OTf, Cs_2CO_3, DMSO, 170 °C, 5 min, 33%.

Scheme 2.

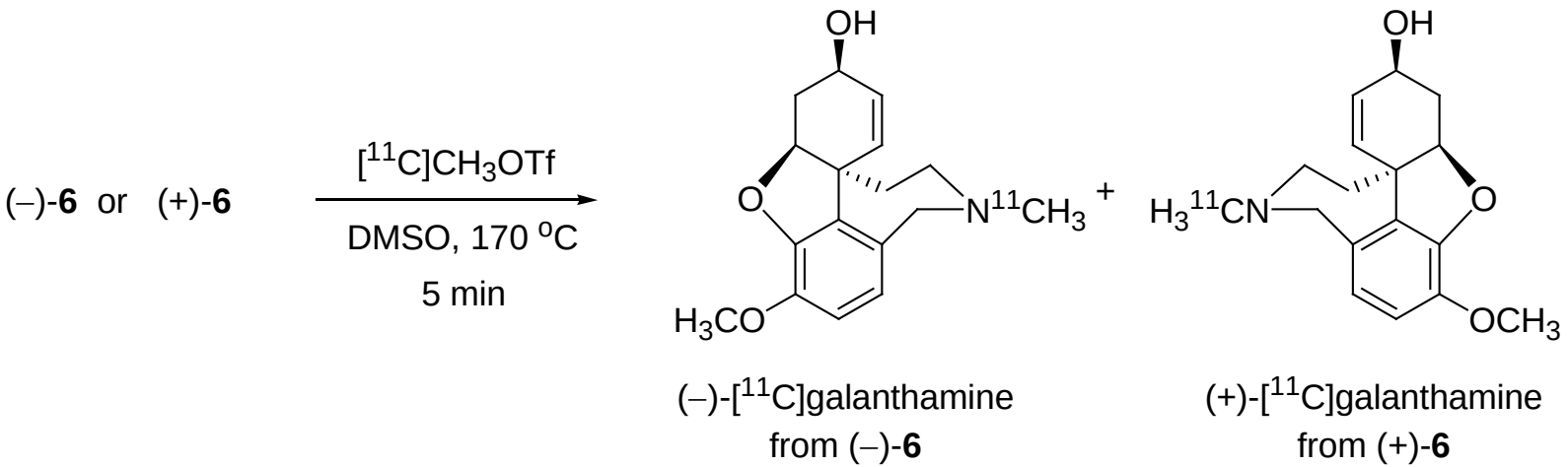

(–)-[^{11}C]galanthamine
from (–)-**6**

(+)-[^{11}C]galanthamine
from (+)-**6**

Table 1.

Table 1. AChE inhibitory activities of (−)- and (+)-galanthamine.

	Inhibition (%)
(–)-galanthamine	94 ± 2.7
(+)-galanthamine	10 ± 4.4
galanthamine·HBr from *Lycoris* sp.	95 ± 1.0

n = 3.